Multiscale shape analysis of particles in 3D using the calypter

Eric PIRARD, Arnaud CALIFICE, Angelique LEONARD and Max GREGOIRE
Universite de Liege, Sart Tilman B52, 4000 LIEGE

Abstract

Shape analysis of particles is a complex issue that cannot be fully addressed with a simple parametric approach. If aspect ratios (elongation, flatness) and convexity indices allow for global characterisation of the form of an object, it becomes obvious that multiscale analysis techniques are required to address the proper characterization of local shape features such as roughness, bluntness, angularity, etc.
Fourier transforms, wavelet transforms, fractal analysis and mathematical morphology are among the most popular multiscale decomposition techniques used in 2D. In this paper we propose the 3D extension of a Euclidean skeleton descriptor called calypter and show how this opens the way to sensitive and robust shape analysis of individual particles in 3D.

Keywords : mathematical morphology, opening, shape

Introduction

Particulate materials are ubiquitous in industrial processes and deserve much attention because of the unique physical properties observed in this specific state of matter. Despite many attempts, the prediction of particulate systems behaviours is still in its infancy. Simulation tools such as the discrete element modelling (DEM) approach have broken new frontiers with the development of 3D models, but they still struggle to take into account realistic shapes and to deal with a sufficiently large number of particles (Cleary and Sawley, 2002).
As an alternative and complement to simulation, advanced characterization of individual particles is a promising tool. The development and acceptance of image analysis based instruments in the recent years has opened the way towards a better understanding of underlying correlations between size/shape characteristics and some fundamental physical properties such as flowability, compactness, dissolution, abrasiveness, etc. With the advent of 3D imaging techniques a major step is being taken towards the definitive characterization of individual particles.

3D single particle imaging

A partial or a full 3D image of an individual particle can be obtained from a series of techniques involving different principles ranging from laser triangulation and stereoscopy to computerized tomography. This last technique is particularly popular since the advent of affordable desktop X-Ray tomography instruments, not to mention the higher resolution XRay CT images that can be acquired at various synchrotron facilities around the world. All the examples included in this paper come from desktop X Ray tomography (Skyscan 1172) of metal powder particles dispersed into a PVC powder medium. The digitization corresponds to an average resolution of the order of 5 000 voxels per individual particle. Particle segmentation has been performed using a simple density thresholding procedure.
The 3D binary image of a particle is defined on a systematic cubic grid with three orthogonal axes (x,y,z) and is composed of voxels having the following attributes:

$$I(x,y,z) = \begin{cases} 1 & \textit{if the voxel belongs to the particle} \\ 0 & \textit{otherwise} \end{cases}$$

The elementary cubic volume associated to each voxel being given by:

$$\Delta V = \Delta x.\Delta y.\Delta z$$

From the raster image, several size and shape features (volume, Feret diameters, inertia moments, etc.) are already accessible as has been showed by several authors (Lin and Miller, 2005; Parra-Denis et al., 2007), but more advanced analytical tools require further pre-processing of the data based on neighbourhood configurations.

Euclidean Distance Transform (EDT)

The Euclidean Distance Transform is one of the most powerful pre-processing tools. It has been introduced by Danielsson (1980) and has since then found many applications in geographical information systems, in image segmentation, etc. The EDT attributes to each pixel of an object its distance (in Euclidean terms) to the closest background pixel. The original algorithm suggested by Danielsson made use of four raster scans, but recent developments have introduced sequential algorithms relying on Voronoi diagram construction that allow to generalize the principle to arbitrary dimensions (Maurer et al., 2003).

From a theoretical point of view, the EDT bears a perfect analogy to the erosion operator in mathematical morphology because it attributes to each voxel the radius of the largest sphere, centred on it, that does not contain any background voxel. The result of an erosion with a perfect sphere of radius (size) λ is given by thresholding the EDT at value $\lambda+1$. It is essential to realize that Euclidean erosions cannot be obtained through iteration of an elementary structuring element because of the non-homothecy of concentric spheres on a cubic grid (figure 1). Using the EDT as an intermediate for computing the eroded set is a necessary step when aiming at morphometry of objects because it eliminates spurious artefacts that would otherwise affect the shape measurements.

Plotting the volume of the 3D EDT as a function of the threshold (λ) is interesting whenever the understanding of how an isotropic front propagates makes sense (e.g. simple analogy with a dissolution front). But, the EDT has more to offer when further processing is performed. This has already been noted by many authors who have been using the EDT as a support function for the extraction of skeletons and other powerful shape descriptors.

Meyer (1989) has shown how the search for crest points followed by homotopic reconstruction could be a way to obtain the skeleton of a shape from a distance function. Ogniewicz and Ilg (1992) suggested alternate ways to obtain Euclidean skeletons by making use of Voronoi transforms. This approach provided accurate skeletons together with efficient tools for a hierarchical classification of skeleton branches. At about the same time, Pirard (1993) suggested a different approach making use of the EDT to locate the centre of each maximum inscribed disc associated to a point of the contour. The strength of this approach was to store the skeleton information together with the contour chain into a single descriptor called calypter (Pirard, 1994). This eliminated the need to handle a large number of skeleton branches and to memorize their complex branching patterns.

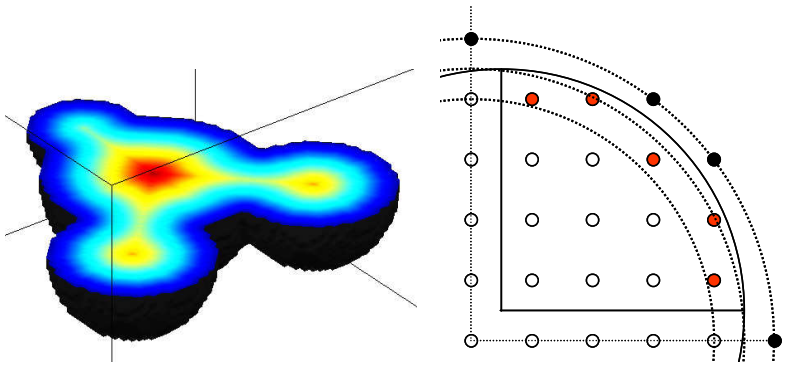

Figure 1 Section through a 3D Euclidean distance transform.
Digitization on a square grid limits the set of discriminable discs. Red pixels correspond to the difference between concentric discs of radius 3 and 4, but they could as well belong to a disc of radius 3 whose center is shifted in x and y by half a grid spacing.

Holosphere Opening Transform (HOT)

The principle of the 2D calypter computation is to proceed from each pixel of the contour by following the steepest path along the EDT and checking whether the corresponding pixel could be the centre of a maximum inscribed disc containing the original contour pixel. Because of image depth limitations, the original calypter algorithm was implemented using an EDT rounded-up to the next integer. The final result is a coding of any shape into the set of its maximum inscribed discs, with the constraint that these discs have integer radii and are centred on the discrete grid. Hence, the more appropriate notion of Holodisc Opening Transform (HOT). In practice, it can be shown that the lack of precision from using a HOT rather than a strictly Euclidean opening transform is rather limited. Considering the added uncertainty about the true position of the centre of a disc, a half grid spacing shift in x and y means an uncertainty of 0.707 on the Euclidean distance measure within a single quarter (figure 1).

The extension of the calypter in 3D is theoretically straightforward as it suffices to associate to each voxel of the surface the corresponding centre of the maximum inscribed sphere (MIS) that does contain this voxel. In practice, the 3D calypter structure will be less handy because the surface voxels have to be triangulated and mapped into a 2D structure that preserves their spatial relationships. MIS centres are identified using a propagation pass analogue to the one developed in 2D. At each step, one out of three different neighbourhood configurations has to be considered depending upon the progression direction (figure 2). The initial progression direction being taken from a discrete approximation of the normal to the surface at the initial surface voxel (x_s,y_s,z_s).

Propagation proceeds towards the local maximum of the EDT in the propagation front. If there is no strict maximum, the progression front is split into two separate paths oriented perpendicularly before definitely stopping. This last exception is required to deal with situations analogue in 3D to a locally horizontal 2D crest perpendicular to the propagation front (e.g. saddle zone).

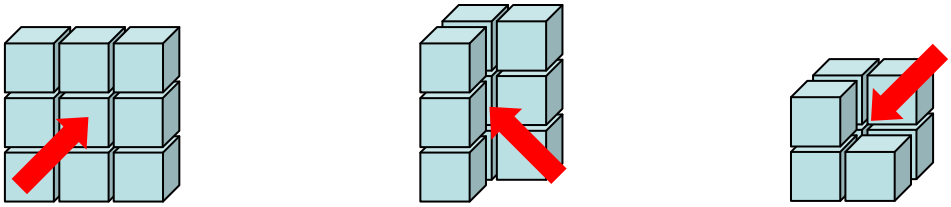

Figure 2 Neighbourhood configurations to be considered for the propagation path on the Euclidean Distance Transform (a) along the edges of the cubic grid, (b) in a face diagonal direction or (c) in a spatial diagonal direction.

At each step, a test is performed to check whether the corresponding voxel (x_i,y_i,z_i) can be a candidate centre for a MIS including the original surface voxel (x_s,y_s,z_s):

$$\left\lfloor \sqrt{(x_i - x_s)^2 + (y_i - y_s)^2 + (z_i - z_s)^2} + 0.5 \right\rfloor = \left\lfloor \sqrt{EDT(x_i, y_i, z_i)} + 0.5 \right\rfloor$$

In other words, the value of the EDT transform at the candidate voxel (EDT(x_i,y_i,z_i)), is checked against the Euclidean measure of distance between the candidate voxel (x_i,y_i,z_i) and the surface voxel (x_s,y_s,z_s). The test is done by using the holosphere metric. The resulting set of maximum inscribed spheres or holosphere opening transform (HOT) is illustrated in figure 3.

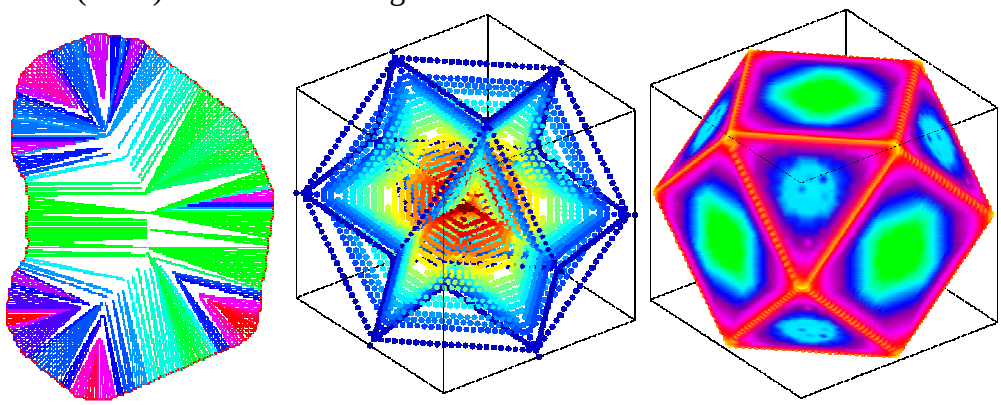

Figure 3 2D calypter of a diamond particle visualising the maximum inscribed disc radii and 3D calyptre of a synthetic cuboactahedron shown as MIS centres or surfaces

Through a different approach, Delerue et al. (1999) developed a Voronoi skeletonization followed by iterative computation of maximum inscribed spheres to analyse the hydrodynamic properties of soils. Because the EDT algorithm by Maurer et al. (2003) is using ordered propagation rather than raster scanning, it should be possible to integrate the identification of the MIS into the Voronoï propagation itself and thereby optimize the computation time.

3D size and shape analysis

Size

Strictly speaking, a size parameter is a dimensional measure that is independent of the notion of shape. This is best formalized by Lebesgue's measure in 3D corresponding to the integration of the particle volume by summing up the individual elementary voxel volumes whose centre belong to the particle:

$$V = \Delta V \sum_{x,y,z} I(x, y, z)$$

Because most applications are used to deal with size expressed as a linear measure, it is tempting to suggest using an equivalent sphere volume diameter:

$$d_V = \sqrt[3]{\frac{6.V}{\pi}}$$

This measure however does not correspond to any physical dimension of the real particle (unless it is a sphere) and is also very sensitive to particle agglomeration. Therefore, an alternative choice is to use the diameter of the maximum inscribed sphere (d_{IN}) which is obtained from the maximum of the EDT as a measure of size. This value is best plotted in a cumulative histogram weighted by volume (fig. 4) and can be of particular interest for a better understanding of dissolution/reaction since it is, in a first approximation, the thickness of a particle that most controls these mechanisms.

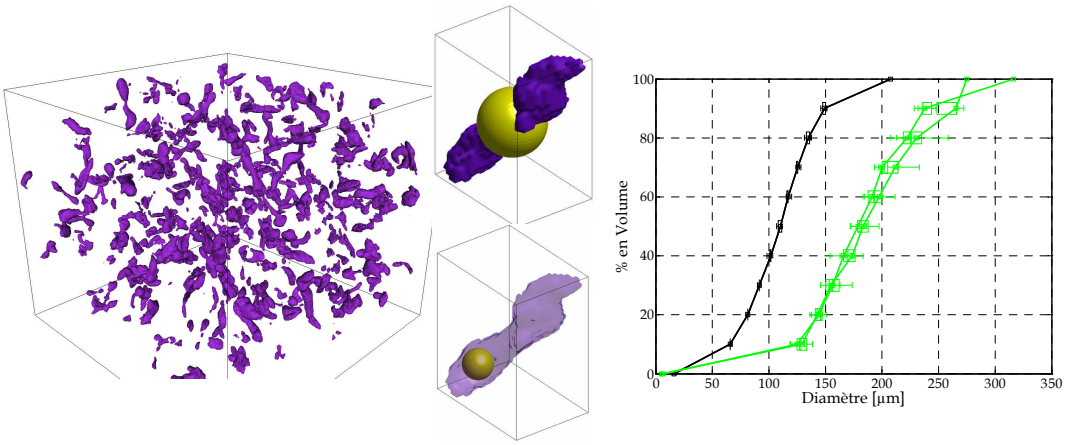

Figure 4 X-Ray CT binary image of a sample of tortuous metal particles. Visualisation of the equivalent volume sphere and the maximum inscribed sphere (d_{IN}). Cumulative distribution by volume of the particle thickness (d_{IN}) in black vs. the particle width in green.

Roughness and bluntness

The similarity between opening and abrasion has been noted by many authors and has been used in particular to try to automate the widespread morphoscopical chart of Krumbein (1941). First attempts by Frossard (1978) were limited by the severe artefacts generated by iterated hexagonal opening functions. In order to overcome this, Pirard (1993) suggested to make use of the calypter and suggested an index (called here bluntness index) computed as follows:

$$W_V = \frac{1}{\sqrt{\overline{V}} - 1} \quad with \quad \overline{V} = \frac{1}{N} . \sum_{i=1}^{i=N} \left(1 + \frac{\lambda_E}{\lambda_i} \right)^2$$

With λ_E corresponding in 3D to d_{IN} and λ_i designating the maximum inscribed disc (sphere in 3D) containing the i^{th} point of the contour.

More recent work by Drevin and Vincent (2002) has again studied the analogy between Euclidean openings in 2D and Krumbein's chart. But, instead of computing a specific index, they have tried to make use of the full granulometry by opening.

One of the strength of the bluntness index is its robustness against digitization conditions. Figure 5 shows the evolution of the bluntness of three simple shapes as a function of the number of voxels. A sensible difference is clearly measured at a resolution of only 5000 voxels per particle!

Conclusion and perspectives

Euclidean mathematical morphology tools on cubic grids have been implemented to address shape analysis of individual particles in 3D. These tools are available for fast and accurate analysis of large amounts of particles and can be tailored to address the specific needs of a better understanding of some physical behaviours such as dissolution, abrasiveness, compactness, etc.

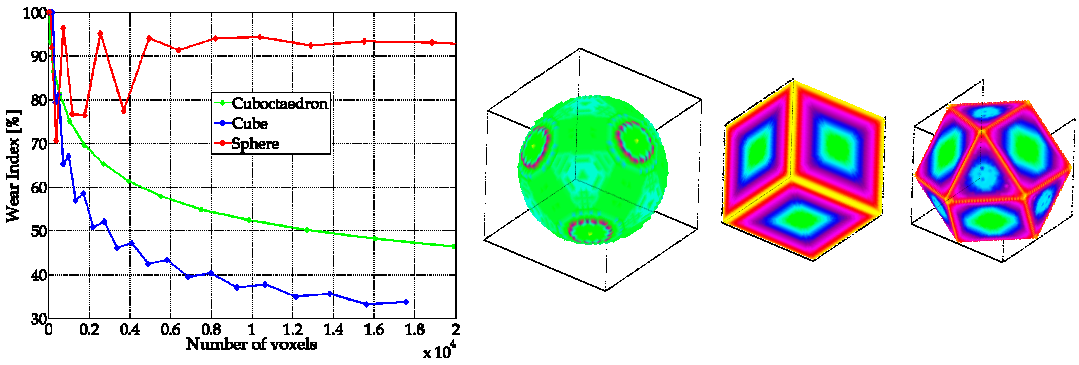

Figure 5 Bluntness index as a function of the number of voxels for three simpe shapes (sphere, cube and cuboctahedron).

Robustness and superior sensitivity of mathematical morphology based methods with respect to other multiscale analysis methods such as Fourier and Fractal has not been demonstrated in this limited application but from 2D experience it is expected that Mathematical Morphology has superior discrimination potential at practical resolutions of 5000 voxels per particle.

Further work on crystallinity and computation of angles between crystal facets is ongoing.

References

Lin CL, Miller JD, (2005). 3d characterization and analysis of particle shape using x-ray microtomography. Pow Tech. 154: 61-9.

Parra Denis E, Barrat C, Jeulin D, Ducottet C (2007). 3d complex shape characterization by statistical analysis: application to aluminium alloys. Mater. Charact. 59: 338-43.

Maurer CR, Qi, R, Raghavan V (2003). A linear time algorithm for computing exact euclidean distance transforms of binary images in arbitrary dimensions. IEEE Trans. on Pattern Anal. and Mach. Intel. 25:265-70.

Delerue JF, Perrier E, Yu ZY, Velde B (1999). New algorithms in 3D image analysis and their application to the measurement of a spatialized pore size distribution in soils. J Physics Chemistry Earth, 24(7):639-44

Cleary PW, Sawley ML (2002), DEM modelling of industrial granular flows: 3D case studies and the effect of particle shape on hopper discharge. Applied Math Modelling 26: 89-111.

Meyer F (1999). Skeletons and perceptual graph. Signal Processing 16: 335-363.

Ogniewicz R, Ilg M, (1992). Voronoi skeletons: theory and applications, in Proc. Conf. on Computer Vision and Pattern Recognition, Champaign IL.

Pirard E, (1993). Morphometrie euclidienne des figures planes. These de doctorat, Univ. Liege, 253pp.

Pirard E, Nivart JF, (1994). New descriptor for skeletons of planar shapes: the calypter. Proc. SPIE, 2180: 248-259

Frossard E, (1978). Caracterisation petrographique et proprietes mecaniques des sables, These Univ Paris VI-Ecole Nat Sup des Mines Paris.

Krumbein WC, (1941). Measurement and geological significance of shape and roundness of sedimentary particles, J Sed Pet. 11(2): 64-72.

Drevin GR, Vincent L, (2002), Granulometric determination of sedimentary rock particle roundness, Proc VI ISMM, 315-325.